applied sciences

MDPI

Article

Compensation for In-Phase/Quadrature Phase Mismatch in Coherent Free-Space Optical QPSK Communication Systems

Xueliang Li [1,*], Tianwen Geng [1], Yucong Gu [1,2], Ruotong Tian [1,2] and Shijie Gao [1]

[1] Changchun Institute of Optics, Fine Mechanics and Physics, Chinese Academy of Sciences, Dongnanhu Road 3888, Changchun 130033, China; gtw@ciomp.ac.cn (T.G.); guyucong@foxmail.com (Y.G.); tianruotong17@mails.ucas.ac.cn (R.T.); gaoshijie@ciomp.ac.cn (S.G.)
[2] University of Chinese Academy of Sciences, Beijing 100049, China
* Correspondence: lxl@ciomp.ac.cn; Tel.: +86-0431-8670-8238

Featured Application: In this paper, we put forward an algorithm switching orthogonalization procedure (ASOP) according to the quality of the in-phase and quadrature signal branches based on the Q value of the eye diagram with less computation. The proposed ASOP scheme can contribute to the frequency offset estimation and phase estimation of free-space optical communication (FSO) systems with turbulence disturbance. Thus, it is hoped that the ASOP scheme we proposed will see the practical application of coherent FSO communication.

Abstract: The Gram–Schmidt orthogonalization procedure (GSOP) and Löwdin symmetric orthogonalization procedure (SYOP) are the two mainstream algorithms for the compensation of phase mismatch in an imperfect optical 90° hybrid. In this paper, we put forward an algorithm switching orthogonalization procedure (ASOP) according to the quality of in-phase and quadrature signals based on the Q value of the eye diagram with less computation. If the quality of the in-phase and quadrature signals has a significant difference, we use the GSOP and select the signal branch with better quality as the initial reference vector for orthogonalization. If they are of about the same quality, then we use the SYOP. We present computer simulations for a coherent free-space optical (FSO) quadrature phase-shift keying (QPSK) communication system and demonstrate the system improvement that can be achieved using the ASOP. Finally, we also show that the proposed ASOP scheme can contribute to the frequency offset and phase estimation of the FSO system in the environment of atmospheric turbulence.

Keywords: coherent communications; free-space optical; IQ imbalance; orthogonalization procedure

Citation: Li, X.; Geng, T.; Gu, Y.; Tian, R.; Gao, S. Compensation for In-Phase/Quadrature Phase Mismatch in Coherent Free-Space Optical QPSK Communication Systems. *Appl. Sci.* **2021**, *11*, 2543. https://doi.org/10.3390/app11062543

Received: 22 February 2021
Accepted: 9 March 2021
Published: 12 March 2021

1. Introduction

Optical coherent detection, in conjunction with electrical digital signal processing (DSP), is considered an essential technology for next-generation optical communication systems [1,2]. Compared to traditional direct detection (DD) systems, coherent detection presents the following advantages [3–5]. First, it has a higher spectrum efficiency and more flexibility to advanced modulation formats such as M-array phase-shift keying (MPSK) and quadrature amplitude modulation (MQAM), followed by conventional direct detection. Second, great sensitivity can be achieved when homodyne detection is used. It also has great potential to be used in free-space communication links with long-range and high-data-rate working scenarios [6,7]. However, the performance of free-space coherent optical communication systems is seriously impaired by imperfections of the systems, such as phase noise induced by the transmitter laser, local oscillator, and wavefront distortion, as well as an imbalance between the in-phase (I) and quadrature (Q) branches in the front end of the coherent optical receiver. In this paper, we mainly focus on the impact of the imbalance between the IQ branches of the quadrature phase-shift keying (QPSK) signal.

The IQ imbalance degrades the system performance severely if left uncompensated in the DSP unit of the receiver. An imperfection in any of the 90° optical hybrids, balanced photodiodes, and transimpedance amplifiers (TIAs) in the front end may introduce an IQ imbalance stemming from the gain and/or the phase mismatch between the IQ branches [8]. Several methods of IQ imbalance compensation in the digital domain have been reported for the QPSK signal [9–15]. The well-known techniques for the orthogonalization of two nonorthogonal vectors are the Gram–Schmidt orthogonalization procedure (GSOP) [10] and Löwdin symmetric orthogonalization procedure (SYOP) methods [11,12]. In [13], compensation is done by the ellipse-correction (EC) method, which is neither applicable to higher-order QAM signals nor effective when the optical signal-to-noise ratio (OSNR) is low. We will explain the above three methods in Section 3. It should be noted that the GSOP is known to depend on the ordering of the initial vector that is meant to be fixed as the reference vector, which is not necessarily a shortcoming for mathematical analysis. It is not an advantage for IQ signal orthogonalization, because if the initially selected vector is of poor quality, then the new vector orthogonal to it is of low quality too. Similarly, the SYOP and EC methods exhibit symmetry and resemblance properties, although the original reference signal is very good. As a result, the quality of the new orthogonal signal may become worse due to the symmetry property.

In this paper, we propose a novel phase mismatch compensation scheme, where the conventional GSOP and the SYOP are modified and combined so as to achieve an optimal orthogonal state between the IQ branches. We mainly study the effects of phase mismatch, which means that the phase difference of IQ signals may be deviated from 90° because of the imperfect optical hybrid. This paper describes the coherent optical communication system under the condition of atmospheric turbulence with a QPSK modulation regime at the rate of 20 Gbps.

2. Channel Statistics and System Structure

2.1. Channel Statistics

In FSO systems, one of the remaining impediments is atmospheric scintillation, which, resulting from the index of refraction fluctuations, can cause fading. The statistics of the strength of scintillation events are generally regarded as following the log-normal distribution. The Rytov variance, ${\sigma_R}^2$, is often used to describe the irradiance fluctuations due to scintillation for the case of weak fluctuations when using the Kolmogorov spectrum for a plane wave [16–18].

$$\sigma_R^2 = 1.23 C_n^2 k^{7/6} L^{11/6} \tag{1}$$

where ${C_n}^2$ is the atmospheric structure constant, which is a measure of the strength of the scintillation. For FSO systems near the ground, it varies from 10×10^{-17} $m^{-2/3}$ to 10×10^{-13} $m^{-2/3}$ according to the atmospheric turbulence condition. $K = 2\pi/\lambda$ is the wave number, and L is the link length. ${\sigma_R}^2 < 1$, ${\sigma_R}^2 \approx 1$, and ${\sigma_R}^2 > 1$ stand for weak-, moderate-, and strong-intensity scintillations, respectively.

The most common channel model for the description of atmospheric turbulence is the log-normal distribution. The distribution of log-amplitude fluctuation is Gaussian. The probability distribution function (PDF) of the received irradiance I is of a log-normal distribution function given by [18]

$$p_I(I) = \frac{1}{I\sigma_R\sqrt{2\pi}} \exp\left\{ -\frac{\left[\ln(I/I_0) + 0.5{\sigma_R}^2\right]^2}{2{\sigma_R}^2} \right\} \tag{2}$$

where I_0 is known as irradiance when there is no turbulence. The phase fluctuation induced by atmospheric turbulence is Gaussian distributed. It is known that the residual phase variance after the modal compensation of the Zernike terms is given by

$$\sigma_\phi^2 = C_J \left(\frac{D}{r_0}\right)^{5/3} \tag{3}$$

where D is the aperture diameter, and r_0 is the Fried parameter, which describes the spatial correlation of phase fluctuations in the receiver plane. For plane waves and Kolmogorov turbulence, r_0 can be expressed in terms of the wavenumber k, C_n^2, and L as $r_0 = 1.68(C_n^2 L k^2)^{-3/5}$ [16,17]. The coefficient $C_J = 1.0299$ in the phase variance assumes that no terms are corrected by a receiver employing modal compensation [19].

2.2. System Structure

The structure of the coherent optical system model is described in Figure 1. In the transmitter, a Mach–Zehnder modulator (MZM) is used to modulate the laser. The in-phase and quadrature branches of the MZM are driven by two electrical pseudorandom binary sequences (PRBSs). The modulated optical signal is amplified by an Erbium-doped fiber amplifier (EDFA) and transmitted over the transmitter antenna.

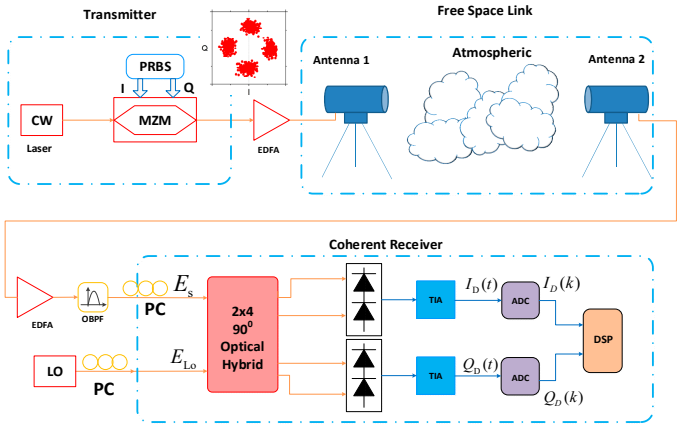

Figure 1. Schematic of a free-space optical communication (FSO) system. CW: continuous-wave laser, MZM: Mach–Zehnder modulator, EDFA: Erbium-doped fiber amplifier, OBPF: optical bandpass filter, PC: polarization controller, TIA: transimpedance amplifier, ADC: analog-to-digital converter, DSP: digital signal processing.

In a coherent receiver, the received optical signal, after passing through the free-space link, is amplified by the pre-EDFA, and a homodyne IQ receiver is used for signal detection. The state of the polarization (SOP) of the local oscillator (LO) and received signal are assumed to be the same by using a polarization controller (PC). The received signal beats with the local oscillator (LO) in a 2×4 90° hybrid, and the output signals are detected by two balanced photodetectors (BDs). The resulting electrical in-phase and quadrature signals are then further processed by high-speed DSP.

3. Theoretical Background and Method

3.1. Phase Mismatch in 90° Optical Hybrid

The 90° optical hybrid is a key component to provide the phase diversity of an optical coherent receiver. It combines two input signals (an incoming signal and a local oscillator reference signal) and generates four optical signals with a 90° phase difference. However, the phase difference of the two output signals may be deviated from 90° when the optical hybrid is imperfect. This quadrature imbalance causes phase errors in the output photocurrents. Phase offset from 90° is called a phase mismatch. There are different ways of modeling the IQ phase mismatch effect. One formalism is to relate a complex signal having phase mismatch imbalance $\{I'(t) + jQ'(t)\}$ with its ideal signal $\{I(t) + jQ(t)\}$ in the form of [2]

$$I'(t) + jQ'(t) = \left[Imb_I I(t) + Imb_Q Q(t)\right] e^{j\left(\frac{\pi}{2} + \phi_{IQ}\right)} \quad (4)$$

where ϕ_{IQ} is the quadrature phase mismatch. The impact of the IQ phase mismatch imbalance for different modulation formats is summarized in [2]. The system performance will degrade significantly if IQ phase mismatch is not compensated.

3.2. GSOP and Löwdin Orthogonalization Compensation Scheme

The GSOP is based on defining a new vector that is orthogonal to the initial vector that makes the two vectors orthogonal, as shown in Figure 2a. Löwdin orthogonalization is a symmetric orthogonalization where both vectors are rotated by the same angle to make them orthogonal, as shown in Figure 2b; on the other hand, the ellipse-correction method finds the least-square ellipse that is best fitted to the constellation of the received signal and then reshapes the ellipse into a perfect circle, as shown in Figure 2c.

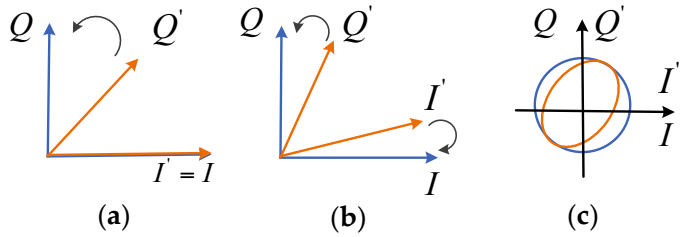

Figure 2. Visual representation of the (**a**) Gram–Schmidt orthogonalization procedure (GSOP), (**b**) Löwdin symmetric orthogonalization procedure (SYOP) and (**c**) ellipse-correction (EC).

The GSOP [10] enables a set of nonorthogonal samples to be transformed into a set of orthogonal samples. Given two nonorthogonal components of the received signal, denoted by $r_I(t)$ and $r_Q(t)$, the GSOP results in a new pair of orthonormal signals, denoted by $I^o(t)$ and $Q^o(t)$, as follows:

$$\begin{bmatrix} I^o(t) \\ Q^o(t) \end{bmatrix} = \begin{bmatrix} \frac{1}{\sqrt{P_I}} & 0 \\ -\frac{\rho}{\sqrt{P_Q P_I}} & \frac{1}{\sqrt{P_Q}} \end{bmatrix} \begin{bmatrix} r_I(t) \\ r_Q(t) \end{bmatrix} \tag{5}$$

where $\rho = E\{r_I(t) \cdot r_Q(t)\}$ is the correlation coefficient, $P_I = E\{{r_I}^2(t)\}$, $P_Q = E\left\{{Q'}^2(t)\right\}$, $Q'(t) = r_Q(t) - \frac{\rho r_I(t)}{P_I}$, and $E\{\bullet\}$ denotes the ensemble average operator.

On the other hand, the Löwdin orthogonalization is a symmetric orthogonalization method where both the vectors are rotated by the same angle to make them orthogonal. The transformation can be written as:

$$\begin{bmatrix} I^o(t) \\ Q^o(t) \end{bmatrix} = \frac{1}{2} \begin{bmatrix} \frac{1}{\sqrt{1+\rho}} + \frac{1}{\sqrt{1-\rho}} & \frac{1}{\sqrt{1+\rho}} - \frac{1}{\sqrt{1-\rho}} \\ \frac{1}{\sqrt{1+\rho}} - \frac{1}{\sqrt{1-\rho}} & \frac{1}{\sqrt{1+\rho}} + \frac{1}{\sqrt{1-\rho}} \end{bmatrix} \begin{bmatrix} I'(t) \\ Q'(t) \end{bmatrix} \tag{6}$$

where ρ is the inner product given as $\rho = \langle I'|Q' \rangle$, $I'(t)$, and $Q'(t)$ are the normalized vectors of $r_I(t)$ and $r_Q(t)$.

3.3. The Algorithm Switching Orthogonalization Procedure (ASOP) Method

As explained in Section 1, the GSOP depends on the ordering of the initially selected reference vector; if the initially selected vector is of poor quality, then the new vector that is orthogonal to it is of low quality too. Similarly, though the Löwdin orthogonalization algorithm and ellipse-correction method exhibit symmetry and resemblance properties, the new orthogonal vectors may be of low quality if one of the initial IQ signals is of high quality or perfect.

Here, we put forward an ASOP scheme according to the quality of the in-phase and quadrature signals based on the Q value of the eye diagram, and the definition of the Q value refers to Equation (7). If the quality of the in-phase signal is better than that of the quadrature signal, we use the GSOP; meanwhile, if the in-phase signal is regarded as the initial reference vector, then we make the other quadrature signal orthogonal to it and vice versa, as shown in Figure 3a,b. If there is not much difference in quality between the IQ signals, such as 10%, for which we use an empirical value that of course can be adjusted

according to the actual effect, we use the SYOP, as shown in Figure 3c. The procedure of ASOP is depicted in Figure 4. It is well to be reminded that the procedure of ASOP is a forward process, does not need feedback, and does this process at the time of system initialization, such that this technique can be implemented with reasonable complexity.

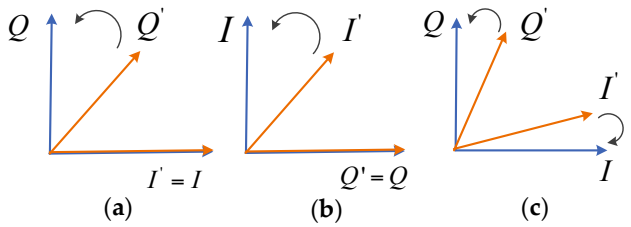

Figure 3. (**a**) Using the in-phase signal as a reference; (**b**) using the quadrature signal as a reference (**c**); using symmetric orthogonalization.

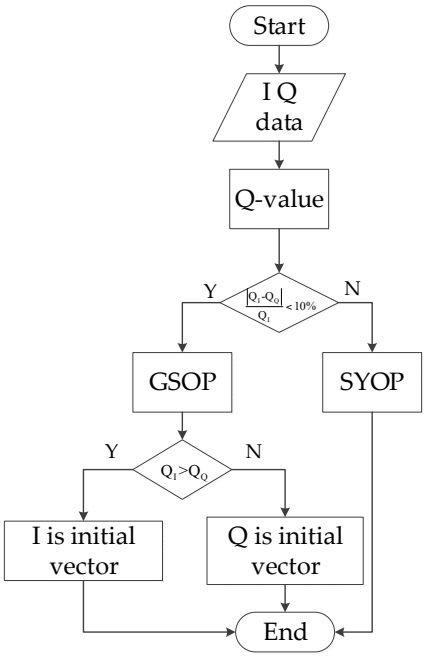

Figure 4. Flow chart of the algorithm switching orthogonalization procedure (ASOP) algorithm.

The criterion for judging the quality of the IQ signal is based on the Q value of the eye diagram and is defined as

$$Q = \frac{\mu_1 - \mu_0}{\sigma_1 + \sigma_0} \tag{7}$$

where μ_1, μ_0, and σ_1, σ_0 are the mean values and standard variance of one and zero levels at the specified sample time. Traditionally, the Q factor metric is well established for on-off keying (OOK) optical systems. A large Q leads to a small bit error rate (BER) [20]. Unfortunately, this metric cannot be simply transferred to QAM signals, where the optical carrier is modulated with multilevel signals both in amplitude and phase. However, for the QPSK modulation scheme, the output amplitudes are +1 or -1 for each of the I or Q branches, so we can calculate the Q factor for the I and Q branches based on the samples of them independently, and the clock recovery is assumed ideal. As shown in Figure 5, the IQ imbalance can lead to an increase in the standard variance of the one and zero levels (σ_1, σ_0) of the received signal eye diagram and then affect the Q factor of the eye diagram, according to Equation (7). Therefore, the value of the Q factor can be used to characterize the IQ imbalance of the signal.

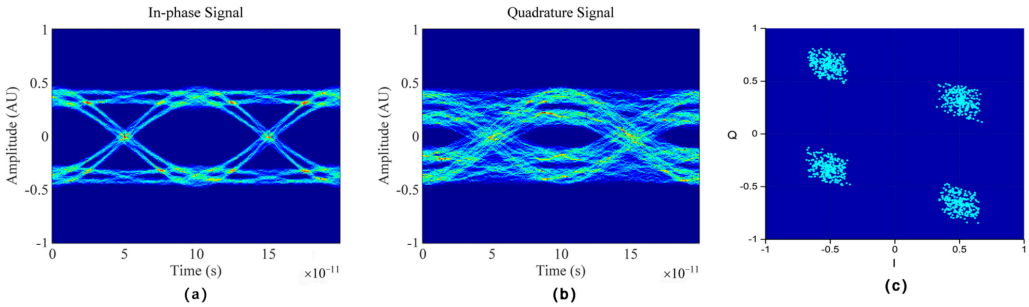

Figure 5. (**a**) In-phase signal eye diagram; (**b**) quadrature signal eye diagram; (**c**) constellation diagram.

For the sake of simplicity, we only show the case that the quality of the in-phase signal is better than that of the quadrature signal. The eye diagram and constellation diagram are illustrated in Figure 5a–c. We can calculate the Q value based on the histogram statistics of Level 0 and Level 1 of the eye diagram. The histogram statistics of the in-phase and quadrature signals are shown in Figure 6. We use Gaussian fitting to calculate the mean and standard variance. As we see in Figure 6c,d, the histogram statistics of the quadrature signal is similar to the bimodal Gaussian distribution. For the convenience of comparison and calculation, we forced Gaussian fitting. The mean and standard variance of Level 0 and Level 1 are listed in Table 1. As we can see, the calculated results of Q value accord with the visual observation of the eye diagram, and in this situation, we should select the in-phase signal as the initial reference vector.

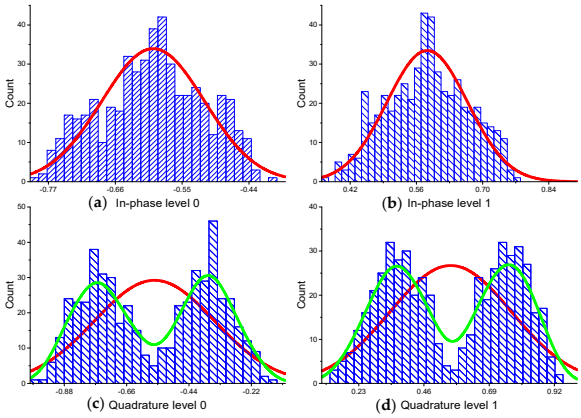

Figure 6. (**a**) In-phase signal Level 0 histogram; (**b**) in-phase signal Level 1 histogram; (**c**) quadrature signal Level 0 histogram; (**d**) quadrature signal Level 1 histogram.

Table 1. Results of histogram statistics.

Branch	Mean	Standard Variance	Q Value
In-phase	$\mu_{I1} = 0.5828$	$\sigma_{I1} = 0.0853$	
	$\mu_{I0} = -0.5976$	$\sigma_{I0} = 0.0844$	$Q_I = 6.9558$
Quadrature	$\mu_{Q1} = 0.5543$	$\sigma_{Q1} = 0.2144$	$Q_Q = 2.5827$
	$\mu_{Q0} = -0.5617$	$\sigma_{Q0} = 0.2117$	

4. Results and Discussion

The simulations were performed with the commercial software tools Virtual Photonics Inc. (VPI) transmission maker and MATLAB to prove the proposed orthogonalization algorithm. Considering the complexity of the atmospheric channel and our practical application scenarios, we chose QPSK modulation format. The wavelength of the laser was 1550 nm, the data rate was 20 Gbit/s (corresponding to 10 Gsymbol/s), and 1 million symbols were simulated using a PRBS sequence. The modulated optical signal was launched into the EDFA, which could amplify the output power to 10 dBm. Then, laser beams

were transmitted in free-space and detected by the PIN balance detector. The resolution of the analog-to-digital converter (ADC) is 8 bits. The optical turbulence parameters are presented in Table 2. As listed in Table 2, the laser beam suffers from a relatively weak scintillation effect. The received optical signal, after passing through the free-space link, was amplified by the EDFA, and the noise figure is 3.5. The samples of the received signals of the I branch and the Q branch are processed by the ASOP algorithm implemented in MATLAB. The constellation diagram and symbol error rate (SER) are estimated.

Table 2. Parameters used in the numerical simulation.

Parameter	Value
Wavelength	1550 nm
Aperture diameter D	5 cm
${C_n}^2$	1.5×10^{-15} m$^{-2/3}$
Transmission distance L	1000 m
Phase variance ${\sigma_\varphi}^2$	0.07 rad
Transmitted power	10 dBm
Received power	−30 dBm
Linewidth	100 kHz
LO power	0 dBm
DSP sampling rate	20 Gsample/s

Figure 7 shows the improvement of the IQ plot (constellation) with the orthogonalization compensation method, including phase noise resulting from the linewidth of the signal laser and LO. The linewidth is set to 100 kHz. We can see that the initial constellations with phase noise and nonorthogonality due to a phase mismatch of 20° (Figure 7a) are improved obviously after the GSOP (Figure 7b), the SYOP (Figure 7c), and the ASOP (Figure 7d). Here, we consider the GSOP as a conventional GSOP using a fixed reference vector (Q signal) and the same in the remainder of this article. The first constellation in the first line represents the situation that the quality of the in-phase signal is better than that of the quadrature signal, so the constellation is improved after the SYOP and further improved after the ASOP because the ASOP selects the right signal as the initial reference vector. Because the phase mismatch is of a small degree, the SYOP can also obtain a good compensation result. As for the GSOP, for the imperfect initial reference vector, the compensated constellation becomes worse. Similarly, the first constellation in the second line represents the situation that the quality of quadrature signal is better than that of the in-phase signal. In this situation, the three compensation methods can all obtain good results because the GSOP also selects the right initial reference vector. The first constellation in the third line represents the situation that the quality of quadrature signal, and the in-phase signal is about the same, but both are not very good. The three compensation methods can all preserve the orthonormal properties of the IQ signals. However, the constellation after the GSOP has rotated a large angle, which may cause performance deterioration. In this situation, the ASOP scheme selects the SYOP algorithm, and the rotated constellations can be further improved by the phase-rotating estimation algorithm.

Figure 8 illustrates the SER performance as a function of the optical signal-to-noise ratio (OSNR/0.1 nm dB) with different ϕ_{IQ}. The shot noise (SN) is included, and the thermal noise (TN) is 10×10^{-12} A/H$\hat{}$(1/2). The linewidth is set to 100 kHz. The 15° of the IQ phase mismatch is already a lot for a commercial device, and in practice, the commercially available coherent receivers have a phase mismatch less than 30°. Thus, we only simulated the range less than 30° in this paper. It is evident that the ASOP and SYOP schemes outperform the GSOP. Here, for the convenience of comparison, we consider the worst case for the GSOP that it always selects the wrong initial reference vector. As shown in Figure 8a, we should note that the results after the GSOP become worse because of the wrong initial reference vector, so the original signal (I) is destroyed undesirably. The green line represents the ideal GSOP, which means that the right initial reference vector is selected. Figure 8b,c shows that the SYOP and ASOP can both improve the SER

performance compared with no compensation of phase mismatch. When the ϕ_{IQ} is less than 5°, the SYOP outperforms the ideal GSOP, so the ASOP scheme applies the SYOP algorithm. This is because of the symmetry and resemblance properties of the SYOP so the noise can be evenly distributed to both the I and Q branches. However, when the ϕ_{IQ} is greater than 5°, the ideal GSOP with the right initial reference vector outperforms the SYOP, so the ASOP scheme applies the GSOP algorithm.

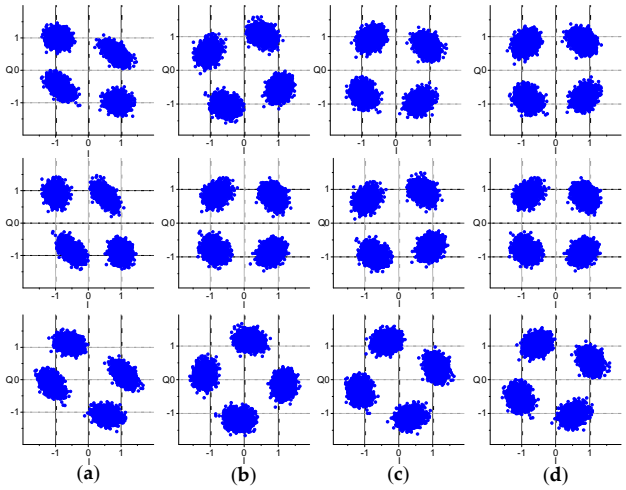

Figure 7. (**a**) Initial constellation; (**b**) after the GSOP; (**c**) after the SYOP; (**d**) after the ASOP.

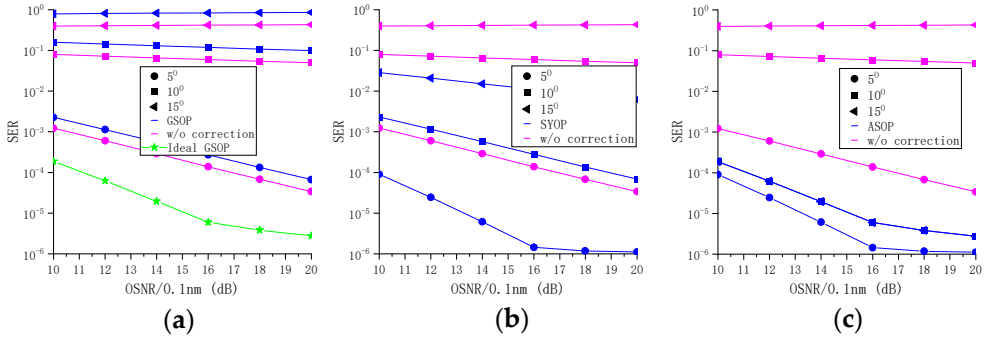

Figure 8. Symbol error rate (SER) versus the optical signal-to-noise ratio (OSNR) with different ϕ_{IQ} of 5°, 10°, and 15° for the (**a**) GSOP, (**b**) the SYOP, (**c**) and the ASOP; W/O: without.

Figure 9 illustrates the SER performance as a function of ϕ_{IQ} with a frequency offset of 400 MHz. The phase drift in the receiver caused by the frequency offset between the transmitter and the local oscillator could be compensated with the carrier frequency estimation algorithm. The carrier frequency estimation was completed by a frequency offset estimation module in VPI with the FFT-based frequency offset estimation algorithm. As we can see, without nonorthogonality compensation, the SER performance of 10×10^{-4} can be obtained only in the rage of 7°. However, a stable SER performance of 10×10^{-6} can be obtained after the ASOP in the range of 20°, and in fact, it can reach a range of 40°. The simulation results also show that the phase mismatch deteriorates the frequency offset estimation effect seriously, so the ASOP also contributes to the frequency offset estimation, thus the system SER performance can be much improved.

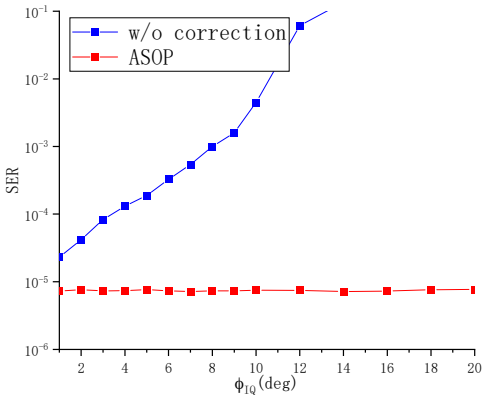

Figure 9. SER versus ϕ_{IQ} with a carrier frequency offset estimation; W/O: without.

In order to verify the impact for the phase mismatch and the compensation effect of the proposed ASOP algorithm, we consider the effects of log-normal amplitude fluctuations and Gaussian phase fluctuations induced by turbulence. The atmospheric structure constant and phase variance are set as $C_n^2 = 1.5 \times 10^{-15}$ $m^{-2/3}$ and $\sigma_\varphi^2 = 0.07$ using Equation (5) in the simulation, which stand for weak atmospheric turbulence condition. As shown in Figure 10, it is clearly shown that the phase fluctuation affects the SER performance seriously without any phase mismatch compensation. We can also see that a stable SER performance of 10×10^{-4} can be obtained after the ASOP in the range of 25°. Instead, the GSOP and SYOP methods can maintain that SER performance only in the range of 5° and the GSOP performed more poorly than SYOP. Within the range of 5°, their performance is about the same due to the M-th power carrier phase estimation scheme we applied [21]. Thus the ASOP can improve the system performance under weak turbulence conditions and when the phase mismatch degree is above 10°, or the phase noise tolerance will be reduced for the phase estimation algorithm.

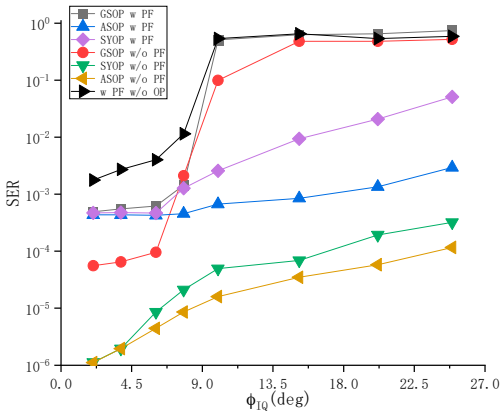

Figure 10. SER versus ϕ_{IQ} with phase estimation under weak turbulence for $C_n^2 = 1.5 \times 10^{-15}$ $m^{-2/3}$. OP: orthogonalization procedure; PF: phase fluctuation; W: with; W/O: without.

In order to further verify the performance of our algorithm under different turbulence intensities and communication distances, we consider the different atmospheric structure constant and communication distance, which stands for weak, moderate, and strong atmospheric turbulence conditions. The parameters used in Table 3 are calculated using Equations (1) and (3). In order to conform to the practical application, the transmitted power in this simulation is 30 dBm. Therefore, the SER of the system will be improved in order of magnitude compared with the previous simulation results. It is clearly shown that with the increase of turbulence intensity, the SER gradually deteriorates. We can also see that the performance of the ASOP algorithm is better than the other two algorithms

under different turbulence conditions, which benefits from its flexible switching between the two algorithms.

Table 3. Parameters used in the numerical simulation, as shown in Figure 11.

C_n^2	L	σ_R^2	σ_ϕ^2	Regime
3×10^{-15}	1 km	0.05	0.15	Weak
8×10^{-16}	10 km	1	0.39	Moderate
6.2×10^{-16}	20 km	3	0.6	Strong

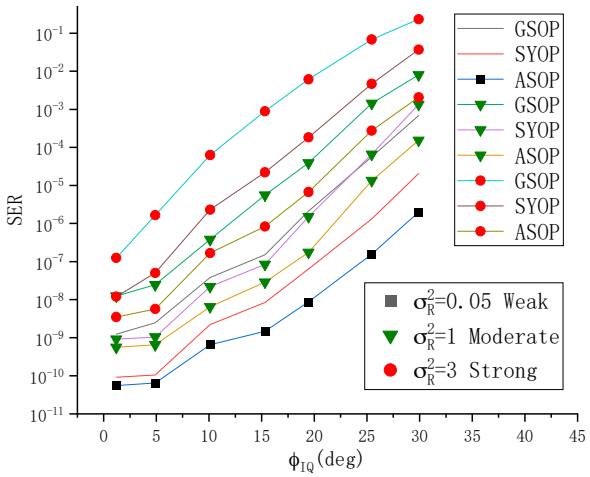

Figure 11. SER versus C_n^2 with phase estimation under different turbulence conditions.

5. Conclusions

In the present work, we investigated the compensation scheme of phase mismatch in an optical 90° hybrid FSO system with a QPSK modulation. The effects of log-normal amplitude fluctuations and Gauss phase fluctuations are also considered. The ASOP scheme is proposed, and the system performance improvement due to this scheme is investigated by simulation. All the simulation results reveal that the ASOP is more powerful than the traditional single GSOP or SYOP schemes. The SER could achieve 10×10^{-6} at the rate of 20 Gbps, and the phase mismatch tolerance can reach 25°. Hence, the ASOP scheme we proposed can contribute to the performance improvement of the FSO system and its practical application.

It should be noted that only the phase mismatch is considered in this paper. Issues such as the development of further optimized algorithms that are suitable for IQ gain mismatch and IQ skew at the same time require further study. In addition, limited by the space and the focus of our team's research, we only simulate the QPSK modulation scheme here; in fact, this algorithm can be used for higher-order QAM modulation, which we do not discuss here.

Author Contributions: Writing—original draft preparation, X.L.; writing—review and editing, X.L.; visualization, Y.G. and R.T.; supervision, T.G.; project administration, S.G. All authors have read and agreed to the published version of the manuscript.

Funding: This research received no external funding.

Institutional Review Board Statement: Not applicable.

Informed Consent Statement: Informed consent was obtained from all subjects involved in the study.

Data Availability Statement: The study did not report any data.

Acknowledgments: This work is supported by the Research Project of Scientific Research Equipment of Chinese Academy of Sciences. The authors also gratefully acknowledge the Optical Communication Laboratory of CIOMP for the use of their equipment.

Conflicts of Interest: The authors declare no conflict of interest.

References

1. Tao, Z.; Li, L.; Liu, L.; Yan, W.; Nakashima, H.; Tanimura, T.; Oda, S.; Hoshida, T.; Rasmussen, J.C. Improvements to Digital Carrier Phase Recovery Algorithm for High-Performance Optical Coherent Receivers. *IEEE J. Sel. Top. Quantum Electron.* **2010**, *16*, 1201–1209. [CrossRef]
2. Faruk, M.S.; Savory, S.J. Digital Signal Processing for Coherent Transceivers Employing Multilevel Formats. *J. Lightwave Technol.* **2017**, *35*, 1125–1141. [CrossRef]
3. Winzer, P.J.; Essiambre, R. Advanced optical modulation formats. *Proc. IEEE* **2006**, *94*, 952–985. [CrossRef]
4. Kikuchi, K. Fundamentals of Coherent Optical Fiber Communications. *J. Lightwave Technol.* **2016**, *34*, 157–179. [CrossRef]
5. Goldfarb, G.; Li, G. BER estimation of QPSK homodyne detection with carrier phase estimation using digital signal processing. *Opt. Express.* **2006**, *14*, 8043–8053. [CrossRef] [PubMed]
6. Niu, M.; Song, X.; Cheng, J.; Holzman, J.F. Performance analysis of coherent wireless optical communications with atmospheric turbulence. *Opt. Express.* **2012**, *20*, 6515–6520. [CrossRef] [PubMed]
7. Belmonte, A.; Khan, J.M. Capacity of coherent free-space optical links using atmospheric compensation techniques. *Opt. Express.* **2009**, *16*, 2763–2773. [CrossRef] [PubMed]
8. Savory, S.J. Digital coherent optical receivers: Algorithms and subsystems. *IEEE J. Sel. Top. Quantum Electron.* **2010**, *16*, 1164–1179. [CrossRef]
9. Faruk, M.S.; Kikuchi, K. Compensation for In-Phase/Quadrature Imbalance in Coherent-Receiver Front End for Optical Quadrature Amplitude Modulation. *IEEE Photonics J.* **2013**, *5*, 7800110. [CrossRef]
10. Fatadin, I.; Savory, S.J.; Ives, D. Compensation of quadrature imbalance in an optical QPSK coherent receiver. *IEEE Photon. Technol. Lett.* **2008**, *20*, 1733–1735. [CrossRef]
11. Löwdin, P.O. On the non-orthogonality problem connected with the use of atomic wave functions in the theory of molecules and crystals. *J. Chem. Phys.* **1950**, *18*, 365–375. [CrossRef]
12. Mayer, I. On Löwdin's method of symmetric orthogonalization. *Int. J. Quantum. Chem.* **2002**, *90*, 63–65. [CrossRef]
13. Chang, S.H.; Chung, H.S.; Kim, K. Impact of Quadrature Imbalance in Optical Coherent QPSK Receiver. *IEEE Photon. Technol. Lett.* **2009**, *21*, 709–711. [CrossRef]
14. Petrou, C.S.; Vgenis, A.; Kiourti, A.; Roudas, I.; Hurley, J.; Sauer, M.; Downie, J.; Mauro, Y.; Raghavan, S. Impact of transmitter and receiver imperfections on the performance of coherent optical QPSK communication systems. In Proceedings of the LEOS 2008-21st Annual Meeting of the IEEE Lasers and Electro-Optics Society, Newport Beach, CA, USA, 9–13 November 2008; pp. 410–411.
15. Petrou, C.; Vgenis, A.; Roudas, I.; Raptis, L. Quadrature imbalance compensation for PDM QPSK coherent optical systems. *IEEE Photon. Technol. Lett.* **2009**, *21*, 1876–1878. [CrossRef]
16. Andrews, L.C.; Phillips, R.L. *Laser Beam Propagation through Random Media*, 2nd ed.; SPIE Press: Bellingham, WA, USA, 2005.
17. Li, M.; Cvijetic, M. Coherent free space optics communications over the maritime atmosphere with use of adaptive optics for beam wavefront correction. *Appl. Opt.* **2015**, *54*, 1453–1462. [CrossRef] [PubMed]
18. Ghassemlooy, Z.; Popoola, W.; Rajbhandari, S. *Optical Wireless Communications: System and Channel Modelling with MATLAB*; Taylor & Francis: Abingdon, UK, 2012.
19. Belmonte, A.; Khan, J.M. Capacity of coherent free-space optical links using diversity-combining techniques. *Opt. Exp.* **2009**, *17*, 12601–12611. [CrossRef] [PubMed]
20. Schmogrow, R.; Nebendahl, B.; Winter, M.; Josten, A. Error vector magnitude as a performance measure for advanced modulation formats. *IEEE Photon. Technol. Lett.* **2012**, *14*, 61–63. [CrossRef]
21. Viterbi, A.M. Nonlinear Estimation of PSK-Modulated Carrier Phase with Application to Burst Digital Transmission. *IEEE Trans. Inf. Theory* **1983**, *29*, 543–551. [CrossRef]